

Post-stack attribute-based fracture characterization: A case study from the Niobrara shale

Geoffrey A. Dorn^{1*} and Joseph P. Dominguez¹ discuss the use of post-stack 3D seismic data to quickly define a relative fracture density attribute and discrete fracture imaging.

Introduction

The ability to determine the relative density and orientations of fractures in potential reservoirs has become increasingly important as resource plays are now a major exploration and development focus for energy companies worldwide. Techniques have been developed using pre-stack data and velocity anisotropy to identify and map fractures. Azimuthal AVO has been employed to estimate fracture density and quantitatively assess how well this approach predicts reservoir quality (Hunt, 2010). Additionally, a new approach to quantitative azimuthal inversion for stress and fracture detection has been developed (Mesdag, 2016). This paper focuses on extracting a relative fracture density attribute and fracture orientations from migrated post-stack 3D seismic volumes.

The detection and mapping of fractures in migrated post-stack 3D seismic data depends on the resolution and signal-to-noise ratio of the data in the seismic volume. A discussion of resolution problems and the limits of resolution in post-stack 3D seismic data, and structurally-oriented post-stack coherent and random noise filtering is followed by descriptions of a Fracture Density attribute and of the extraction of fracture orientations. An example of the results of applying these processes and workflow is included from the Niobrara shale play in the United States.

Types of resolution problems

Resolution is commonly defined as the ability to separate two features that are close together (Sheriff, 2002) – what is called a separation problem. Unfortunately, the limits on resolution for separation problems are often inappropriately applied to other types of resolution problems. This common misunderstanding of the limits of seismic resolution has led many interpreters to question the physical possibility of determining fracture density or imaging fractures in stacked migrated seismic data. A brief discussion of resolution is necessary to understand why detection of fractures is possible in post-stack seismic volumes.

A broader, more complete definition of resolution and detection (Dorn, 1988) is:

- Seismic resolution is the detail that can be interpreted about physical changes in the subsurface:
 - The resolvable limit is the limit at which the geologic change can be quantified
 - The detectable limit is the limit at which the geologic change can be identified but not quantified

There are two key aspects to this definition. First, discussions of resolution often tend to ignore the fact that if an effect is below the level at which a reasonable amount of interpretational confidence can be placed, then that effect is not resolvable for practical purposes. Second, what we are trying to resolve in the subsurface are changes. The objective may be to detect vertical changes in physical properties (layering), changes in size or position, or effects that reflect both structural and lithologic variations – resolution and detectability are not restricted to separation problems.

A list of the various types of resolution problems includes (Dorn, 1988):

- Separation
- Dynamic Range
- Relative Change

Separation problems

Sheriff's aforementioned definition of resolution for separation problems applies to seismic data and interpretations of seismic data in both the time and spatial domains (Herron, 2011). The limit of vertical resolution (the Rayleigh limit) is based on the dominant frequency in the seismic data at a given time or depth, and is derived as $\lambda/4$ where λ is the wavelength of the dominant frequency. Similarly, the spatial resolution of seismic data is described in terms of the Fresnel Zone of the seismic data at a given time or depth. For full 3D migrated data the radius of the first Fresnel Zone is also $\lambda/4$. An assumption is made that the vertical sampling and horizontal sampling of the seismic data are sufficient to satisfy the Nyquist Theorem for the dominant frequency, the steepest reflector, and the area of smallest feature of interest in the survey (Herron, 2011).

This classic definition of resolution pertains to what we will call a Separation Problem. Vertically, it relates to how thin a layer can be and still be observed by the interpreter to have a separate top and base (i.e., it can be perceived as a layer with top and bottom surfaces). Horizontally, it relates to how closely spaced two features can be and still be observed to be two separate features. These are typically referred to as the resolvable limits for vertical and horizontal separation problems.

There are, however, phenomena that enable the interpreter to use seismic data to infer or detect separations vertically and horizontally that are smaller than the resolvable limits. The detectable limits for vertical separation problems, for example

¹ CCG GeoSoftware

* Corresponding author, E-mail: geoffrey.dorn@cgg.com

taking advantage of amplitude tuning effects at thicknesses less than the resolvable thickness, are typically stated as being on the order of $\lambda/8$.

This type of resolution and detection problem (separation problem) has received by far the greatest exposure in the geophysical literature including recent research on improving vertical and spatial resolution and detection in separation problems to $\lambda/25$ (e.g., Bancroft et al., 2005; Pierle, 2009; Zeng, 2014, 2016).

Dynamic range problems

The dynamic range resolution problem refers to the situation where the target signal is a relatively low-amplitude feature in the presence of higher-amplitude features and noise. A dynamic range problem depends on the signal in the seismic data owing to the feature of interest being of sufficient strength to be detectable amid other signal and noise.

Berkhout (1984) demonstrated that the type of wavelet that optimizes the resolution for the high-amplitude doublets does a poor job of resolving the weaker-amplitude events. He also presents a mathematical development of the separation and dynamic range problems in spatial resolution. By developing the concept of a three-dimensional seismic wavelet, resolution can be treated in a consistent fashion mathematically for both vertical and horizontal separation and dynamic range problems.

Relative change problems

A relative change resolution problem is one in which the interpreter is trying to detect and resolve a change in a feature

or event. An example of a relative change problem is shown in Figure 1 (Dorn et al., 1996). In the seismic horizon slice (Figure 1a) dip magnitude is shown in colour, with steep dips shown in pink and shallow dips shown in blue. The locations of several small throw faults are indicated by arrows. Figure 1b shows a seismic section extracted from the volume that is approximately perpendicular to each fault. The reflection of interest is the Top Rotliegend event (shown in red). There is at least one fault in the sequence (number 2) that has no visible offset on this section – the vertical offset is less than one sample. Fault 2 is very easily interpreted, however, from the dip magnitude attribute horizon slice in Figure 1a. The fault can be interpreted with confidence, so using the definition above, it can be resolved. Fault 2 would likely be overlooked on a 2D survey. It is only interpretable here because the interpreter has access to horizon slices (or stratal slices) and can readily see and map the fault on a dip attribute. Experimentation at ARCO in the 1980s demonstrated that in relatively noise-free data, an interpreter could reliably map faults with subsample throws of as little as $\lambda/28$.

All three types of resolution problems are affected by coherent and random noise in the data. The resolution and detectability of a separation problem is degraded by noise. The dynamic range problem is highly dependent on the relationship between the magnitude of the signal of interest and the magnitude of the coherent and random noise present. The relative change problem is very sensitive to noise in the volume that may alter or obliterate the subtle signal of interest.

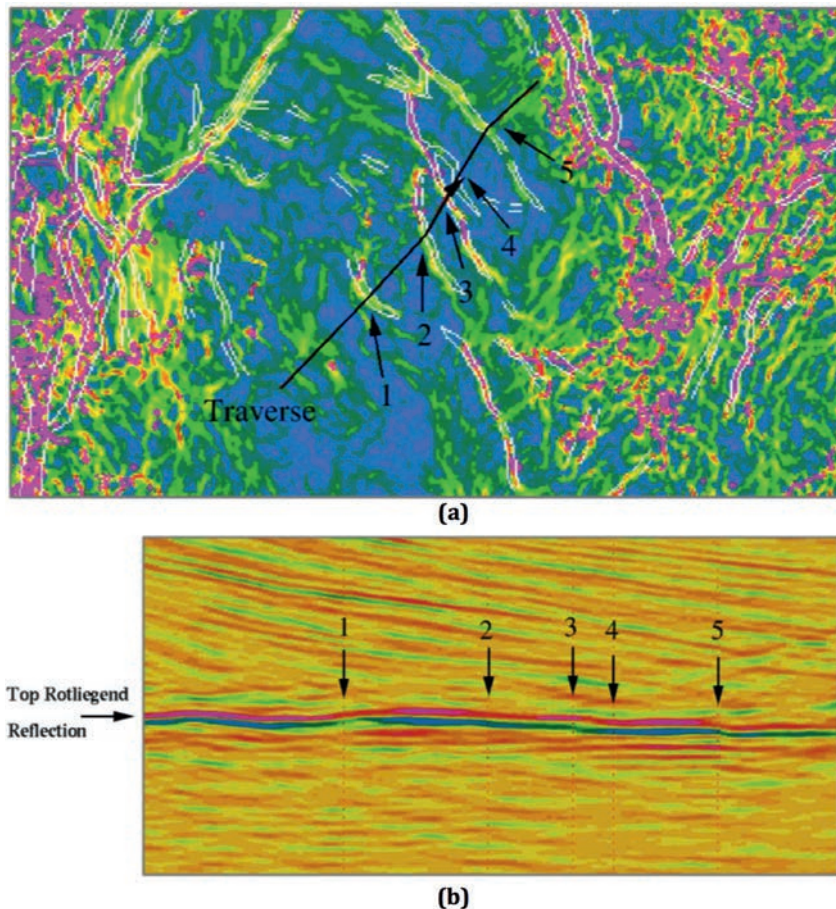


Figure 1 Locations of five example faults at the Top Rotliegend in a survey in the North Sea. Five resolvable faults are indicated on a dip magnitude attribute at the Top Rotliegend reflection (a); the locations of the same five faults are shown on the vertical section (b). The fault labelled '2' shows no visible displacement at the Top Rotliegend event. The displacement on this fault is less than 1 sample in the seismic data, but the fault is easily resolved and interpreted from the dip magnitude attribute.

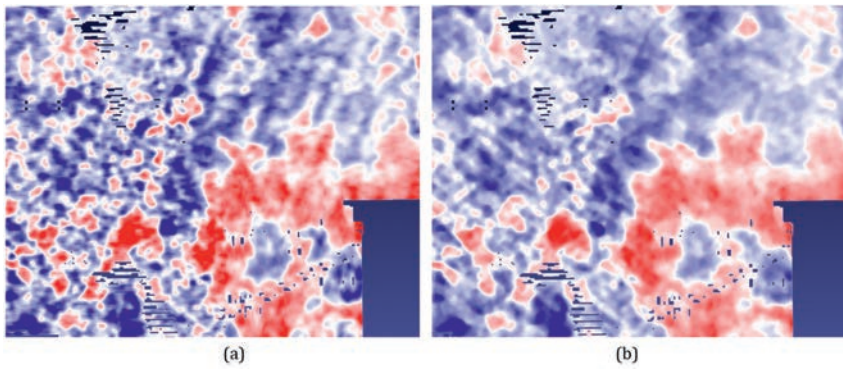


Figure 2 A shallow time slice from the DJ Basin project data showing the raw data (a): the same shallow time slice after data conditioning (b). Ten wavelengths and orientations of acquisition footprint have been removed and then a random noise filter applied.

Detecting the effects of fractures

The workflow used in this study for detection and mapping of fractures in 3D post-stack seismic data includes the following steps:

- Noise Management:
 - Structurally oriented filtering of coherent and random noise from the seismic volume
- Edge Detection
 - Initial imaging of edges in the data using an edge attribute that is dependent only on amplitude change
 - Statistical estimation of relative fracture density based on the edge attribute as input
- Fracture Imaging
 - Imaging of fractures and orientations using the edge attribute as input to a fault and fracture enhancing attribute calculation.

The data used for this study is from the Niobrara Shale in the Denver-Julesburg (DJ) Basin in Colorado, USA.

Noise management

Detection and resolution of fractures and small faults in 3D seismic volumes involves a combination of dynamic range and relative change problems. The interpreter is trying to detect the small signal from fractures and small throw faults in the presence of noise and signals from larger faults, stratigraphic edges and other features in the seismic volume. Detection and resolution of fractures in these volumes depends on minimizing the noise in the seismic volume.

The smaller the physical effect the interpreter is trying to image or quantify in the seismic data, the greater the degree of attention that must be given to filtering noise from the data. In post-stack seismic data both coherent noise (acquisition footprint) and random noise are present to varying degrees.

A structurally oriented footprint removal process based on a destriping algorithm from satellite image processing was used to remove coherent noise from the migrated seismic volume (Dorn et al., 2012). This process was then followed by application of a structurally oriented, edge-preserving median filter for random noise removal. Figure 2 illustrates the results of these data conditioning steps. The time slice in Figure 2a prior to noise filtering clearly shows multiple wavelengths and azimuths of acquisition footprint along with scattered random noise. Analysing the entire volume of interest, footprint was identified in inline, crossline, and oblique orientations. In all, ten wavelengths and orientations of footprint were removed from the data. After applying a structurally oriented

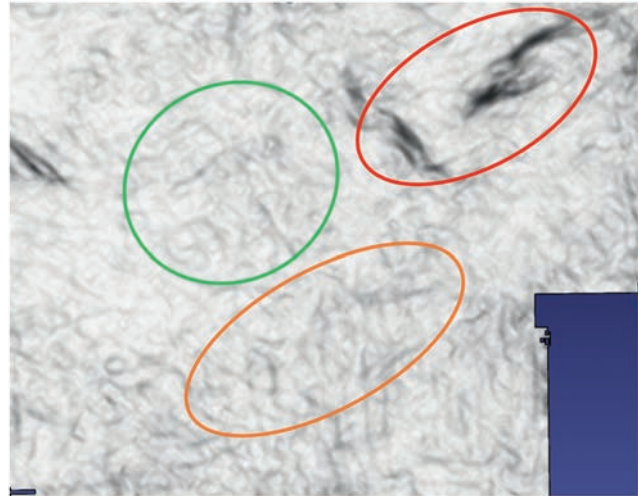


Figure 3 The Fracture detection attribute, a coherence class attribute, requires an amplitude change but does not require any offset and is tunable in the z dimension to allow for detection of subsample discontinuities in the seismic signal. Large throughgoing faults are shown in the red oval, smaller faults in the orange oval, and mostly fracture signal in the light grey within the green circle.

edge-preserving median filter to remove random noise, the final noise-filtered time slice is shown in Figure 2(b).

Edge detection

Physically, the presence of fractures or fracture swarms scatters some of the seismic energy creating an amplitude change that is measured as an indication of fractures.

A discontinuity class attribute, Horizon Edge Stacking (HES) (Dorn et al., 2012), was applied to the noise-filtered seismic volume to perform initial fracture imaging. This structurally-oriented edge attribute does not require any vertical displacement to image a discontinuity. All HES requires is a change in the seismic amplitude between samples on neighbouring traces. This change in amplitude can be quite small if the coherent and random noise has been removed from the seismic volume prior to creating the HES attribute volume.

The larger faults imaged by the HES attribute are shown in Figure 3 as dark black lineaments. The lighter grey data, weaker discontinuities than the large faults, is the data that may be associated with the very small throw faults and fractures. Variations in other properties in the subsurface including lithologic variations, stratigraphic changes, and any remaining noise could also contribute to small-amplitude variations that might also affect the HES attribute. If present, these effects can typically be eliminated

later in the interpretation based on their vertical and horizontal extent, their orientation, and other characteristics that distinguish them from small throw faults and fractures in the area.

Fracture density attribute

The HES attribute volume was then used as input to calculate a volume estimate of fracture density. The process calculates fracture density in 3D using a cube-shaped operator, which is applied at each sample position in the volume of interest. The ratio of the number of samples having edge values in a range specified by the user, to the total number of samples within the cubic operator, is calculated at each point in the volume to create the estimate of fracture density.

An example of a slice through the fracture density attribute for the portion of the Niobrara shale included in this study is shown in Figure 4. If the edge data is associated with small throw faults and fractures, it reveals areas of the highest concentrations of faults and fractures. This attribute volume, calculated early in the workflow, may be useful to identify vertical and lateral key areas of interest, as well as for preliminary well path planning, and could also impact asset team acreage acquisition or release recommendations.

Edge imaging — the Discrete Fracture Network

A Discrete Fracture Network is created from the HES attribute volume using AFE, an advanced fault and fracture imaging process described by Dorn et al., (2012) and based on work orig-

inally described by Crawford and Medwedeff (1999). Using very short windowed radon transforms, the HES volume is processed to create an AFE volume (fault and fracture likelihood) and an associated orientation volume (fault and fracture dip vector volume). The fracture likelihood attribute is called a Discrete Fracture Network (DFN) volume.

An example of the DFN attribute in the Niobrara is shown on a time slice in Figure 5. Throughgoing faults can be isolated by thresholding out the highest likelihood values in the volume at the brightest white end of the DFN attribute range. The smaller faults and fractures occupy the grey scale centre part of the DFN attribute range, and are shown in Figure 5a. The calculation of the DFN attribute also yields fracture strike and dip from the orientation volume.

All of this information is then used to extract fault and fracture planes. In the Niobrara project, a total of 7778 fracture planes were extracted from a small 3D sub-volume of the Niobrara interval. Figure 5b shows only those extracted fault and fracture planes which intersect with the Niobrara D formation surface co-rendered with a nearby seismic time slice. In this workflow large and small throw faults are imaged and extracted. The fracture signals and the resulting extracted fracture planes, down to the detectable limit, represent swarms of fractures and their dominant orientations from specific areas of the 3D seismic volume.

Prior to this study, a Niobrara outcrop fracture characterization and orientation analysis was conducted to provide an analog for improved subsurface reservoir characterization (Grechishnikova, 2016a, 2016b). In her study, Grechishnikova found the following compressional and shear fracture joint set average azimuths in the LIDAR data for the Niobrara:

- J1 set: 345° (compressional)
- J2 set: 259° (extensional)
- S1 conjugate shear set 1: 246°
- S2 conjugate shear set 2: 306°

The data generated in our study produced four clusters with average orientations given by:

- C1: 345°
- C2: 265°
- C3: 243°
- C4: 308°

These strikes of the four clusters of fractures (C1 – C4) obtained from the 3D seismic volume in this study show very close agreement with the four fracture set orientations obtained in the LIDAR study.

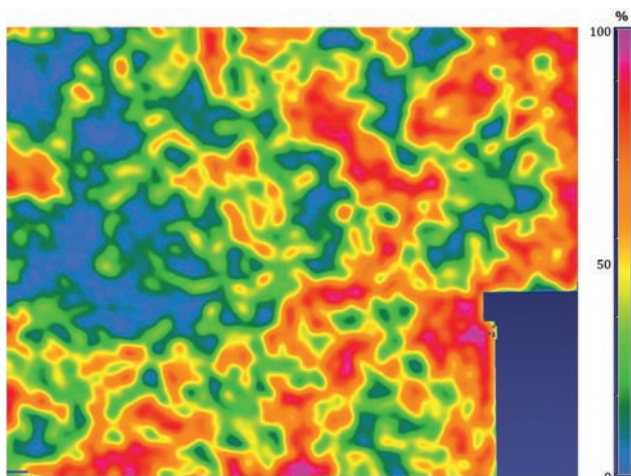


Figure 4 The Fracture density attribute. Throughgoing fault zones and their associated fractures are indicated by the quasi-linear red and magenta areas of high fracture density, while the orange and yellow, somewhat disconnected, regions indicate areas of smaller faults and fracture swarms.

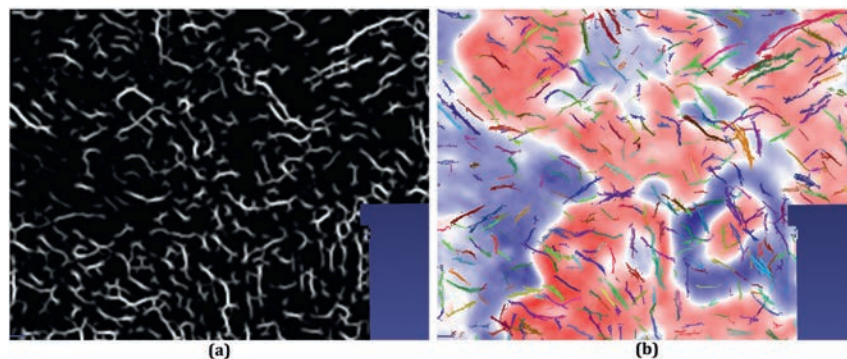


Figure 5 The Discrete Fracture Network attribute is a fault and fracture enhanced volume shown in (a). Throughgoing faults are indicated in the brightest white or high fault probability, while the fractures are indicated in the lighter grey scale. (b) shows extracted fault and fracture planes which intersect the Niobrara D bench surface co-rendered with a nearby seismic time slice.

Conclusions

The limits on resolution for separation problems are often inappropriately applied to other types of resolution problems and this has led many interpreters to question the physical possibility of determining fracture density or imaging fractures in stacked migrated seismic data. This study has employed a workflow based on the premise that the imaging of fractures and small throw faults represents a relative change problem. For this type of problem, with proper noise management, a detectable limit of $\lambda/28$ in post-stack data is feasible. The project work demonstrates that smaller physical effects, such as the amplitude effect owing to scattering by fracture swarms, can be imaged and quantified in the 3D seismic data.

The method requires great attention to filtering noise from the data. These changes in amplitude can be quite small if the coherent and random noise has been removed from the seismic volume prior to creating the fracture detection attribute volume. The fracture detection attribute measures the scattering of seismic energy caused by the presence of fracture swarms and forms the basis for all subsequent calculations. While this attribute is non-unique, when computed after rigorous data conditioning, the fracture signal can be confidently measured and information extracted which correlates well with detailed surface observations and identifies a similar DJ Basin stress field in the subsurface data.

Finally, this post-stack workflow provides extracted seismic information which can positively impact fractured reservoir exploration and development decisions.

Acknowledgements

We thank our CGG colleague Jon Downton for reviewing this paper and CGG for permission to publish this information. We would also like to thank SEI Seismic Exchange for access to the DJ Basin project seismic volume and permission to show this information. The seismic data and seismic data processing was provided by Echo Geophysical Corporation (now SEI); interpretation is that of the authors. All project work was performed using CGG Geo-Software's InsightEarth advanced seismic interpretation software.

References

Bancroft, J.C., Guirigay, T. Isaac H., and Saeed, H. [2015]. Processing seismic data for high spatial resolution. *SEG Annual International Meeting*, Expanded Abstracts, 4201-4205.

- Berkhout, A.J. [1984]. *Seismic resolution: a quantitative analysis of resolving power of acoustical echo techniques*. Geophysical Press, London.
- Crawford, M.F. and Medwedeff, D.A. [1999]. *Automated Extraction of Fault Surfaces from 3-D Seismic Data*. US Patent 5,987,388.
- Dorn, G.A. [1988]. Vertical and Horizontal Resolution of 3D Seismic Surveys. *Norwegian Petroleum Society Meeting on Resolution*, Expanded Abstracts.
- Dorn, G.A., Tubman, K.M., Cooke, D. and O'Connor, R. [1996]. Geophysical reservoir characterization of Pickerill Field, North Sea, using 3-D seismic and well data. In: Weimer, P. and Davis, T.L. (Eds.) *Applications of 3-D Seismic Data to Exploration and Production*, AAPG, 107-121.
- Dorn, G.A., Kadlec, B. and Murtha, P. [2012]. Imaging Faults in 3D Seismic Volumes. *SEG Annual International Meeting*, Expanded Abstracts.
- Grchishnikova, A. [2016a]. Integrated application of a high-resolution LIDAR outcrop survey of an unconventional Niobrara Reservoir, Denver Basin, Colorado. *First Break*, **34**, 65-71.
- Grchishnikova, A. [2016b]. Discrete Fracture Network Model developed from a High Resolution LIDAR Outcrop Survey of a Naturally Fractured Unconventional Niobrara Reservoir, Denver Basin. *Unconventional Resources Technology Conference (URTeC)*, Expanded Abstracts.
- Hunt, L., Reynolds, S. Brown, T., Hadley, S., Downton, J. and Chopra, S. [2010]. Quantitative estimate of fracture density variations in the Nordegg with azimuthal AVO and curvature: A case study. *The Leading Edge*, **29** (9), 1122-1137.
- Herron, D.F. [2011]. First Steps in Seismic Interpretation, *Geophysical Monograph Series*, Society of Exploration Geophysicists.
- Mesdag, P. [2016]. A new approach to quantitative azimuthal inversion for stress and fracture detection. *SEG Annual International Meeting*, Expanded Abstracts.
- Pierle, T.A. [2009]. Seismic Resolution: Thinner than first believed. *SEG Annual International Meeting*, Expanded Abstracts, 1014-1019.
- Sheriff, R.E. [2002]. *Encyclopedic Dictionary of Applied Geophysics*. Society of Exploration Geophysicists.
- Zeng, H. [2014]. Spatial Resolution of Stratal Slice and Its Implications. *SPG/SEG Beijing 2014 International Geophysical Conference*, Expanded Abstracts, 947-950.
- Zeng, H. [2016]. Phase unwrapping for thin-bed seismic chronostratigraphy below seismic resolution limit. *SPG/SEG Beijing 2016 International Geophysical Conference*, Expanded Abstracts, 552-555.